

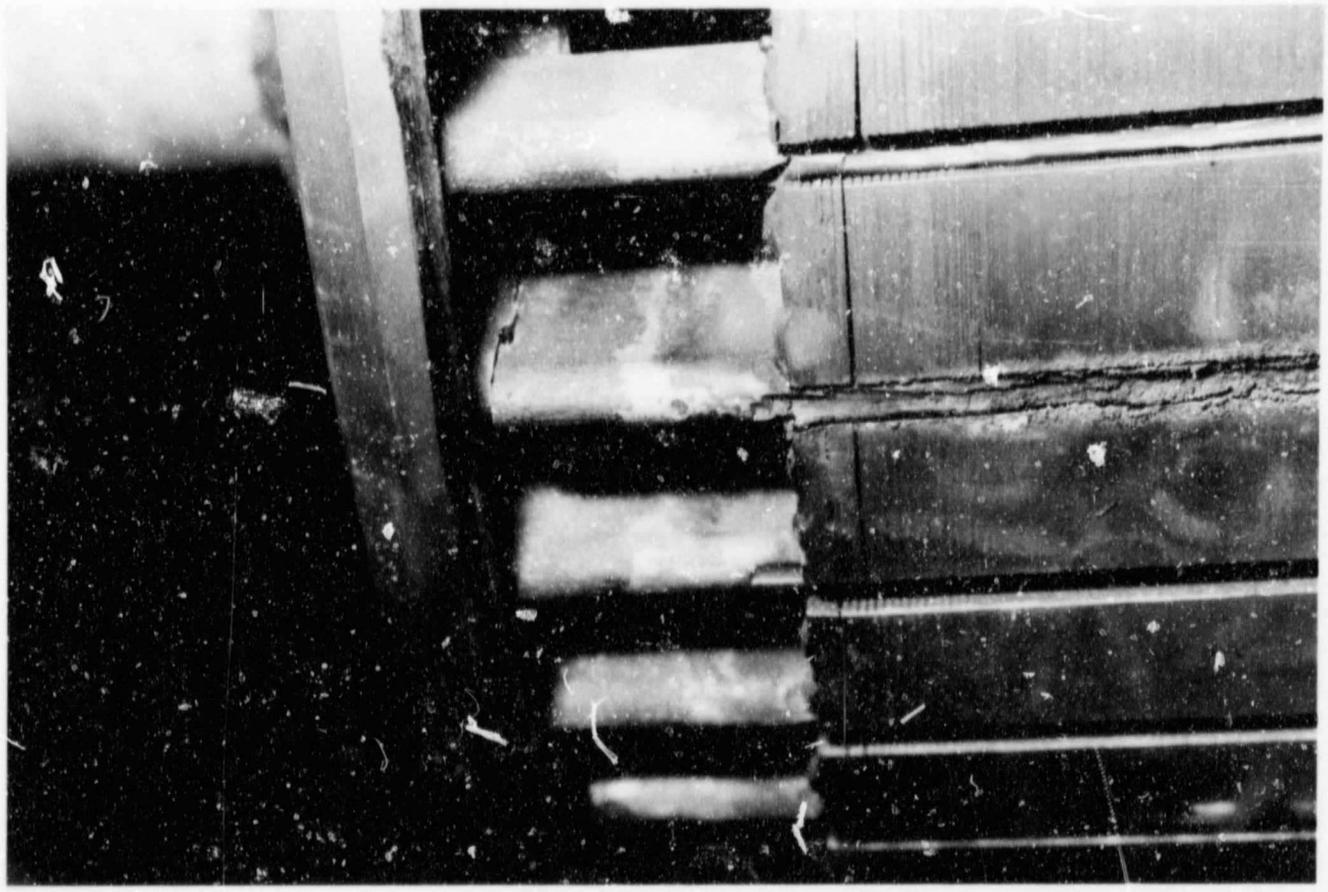
https://dspace.org/

Vibration analysis and diagnostic techniques, with reference to the Implementation of a vibration condition monitoring programme.

Ducci, P P

2015-01-20
http://hdl.handle.net/10539/16617

Downloaded from a DSpace repository. https://dspace.org/



ROTOR BAR DEFECTS IN INDUCTION MOTORS

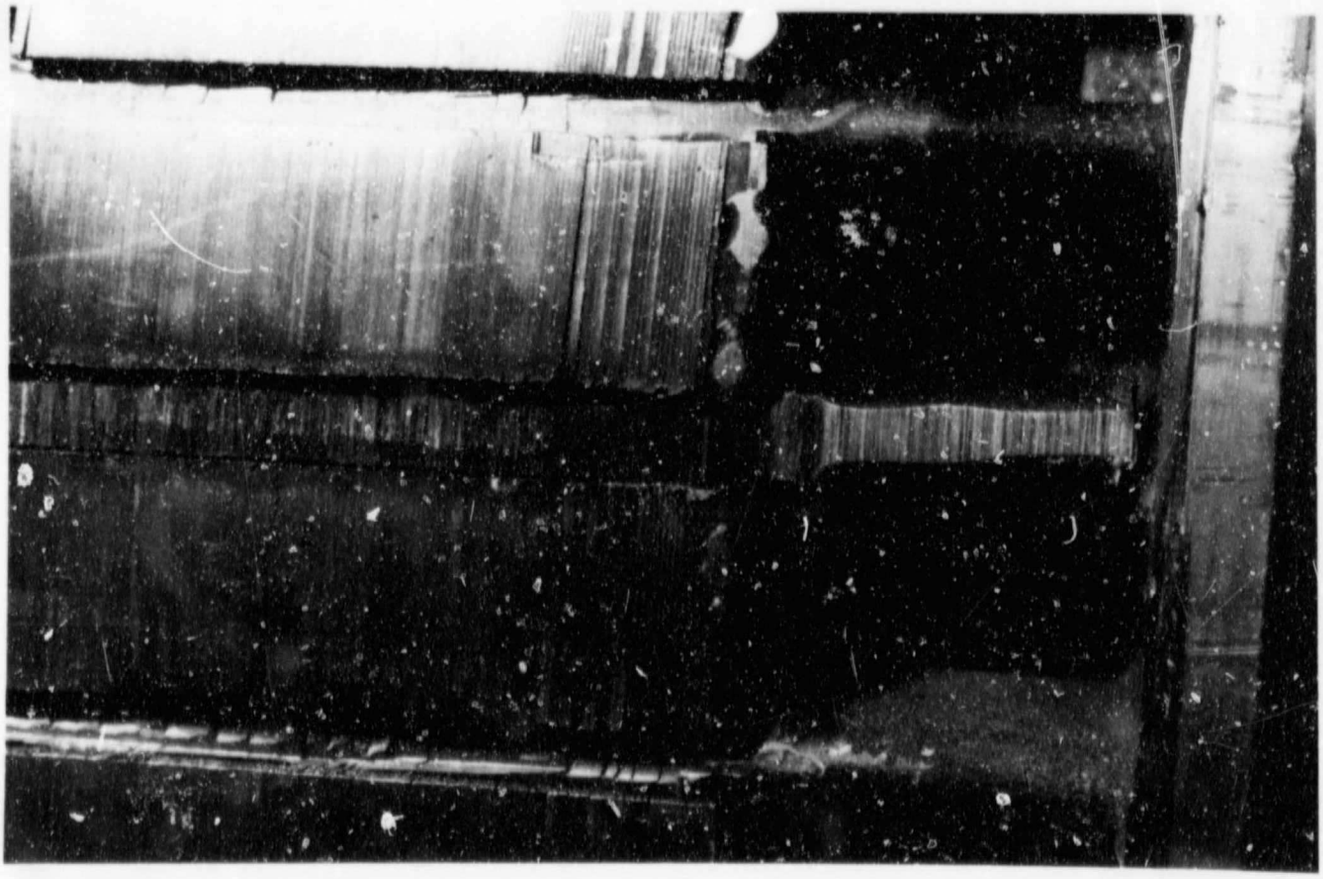


FIGURE 6.7

6.7.2 Theory

6.7.2.1 Vibration

A very common fault with squirrel cage induction motors is that of broken bars near one end ring. When this occurs substantial inter-bar currents may exist between the broken bar and adjacent bars. The current is more concentrated at the end where the bar is broken. The inter-box currents flow tangentially from the broken bar to the adjacent bars and consequently they establish axial fluxes as shown in Figure 6.8. This gives rise to four axial poles which are not symmetrically located around the circumference. Due to the inevitable changes in the permeability that these four poles will encounter with each revolution of the rotor, a four times running speed vibration component is produced with a large modulation at twice slip frequency. The slip frequency is defined as the difference between line synchronous frequency and motor speed. Landy (33).

This four times running speed vibration component will be totally current dependent. This means that if a broken bar exists, then the 4 x RPM axial vibration of the motor must increase with load due to the associated increase in the rotor currents.

6.7.2.2 Current (Hargis et al (34))

It may be shown that if a contiguous group of bars subtending electrical angle is open circuit, and the machine speed remains constant,. the ratio of the magnitude of this component to current to that of supply current is given approximately by:

$$R_s \approx \text{Sin}(\alpha)/2p(2\pi - \alpha)$$

where $\alpha = 2\pi np/N$

p = number of pole pairs

N = number of slots

n = number of broken contiguous bars

$n \ll N$

This cyclic variation in current produces a torque variation at twice slip frequency. This results in a speed variation dependent upon the system inertia, which is generally not negligible. Consequently there is a reduction in the magnitude of the current component at w(1-2s) and a component appears at w(1+2s), enhanced by modulation of the third time-harmonic flux in the stator, Where s represents slip.

The stator current inherently reflects the overall condition of the rotor, and is not capable of providing information on the configuration of non-contiguous broken bars.

Present slip is defined as $(w_f - w_r)/w_f \times 100$
where w_f = synchronous speed of the rotating field.
w_r = speed of the rotor.

For a typical induction motor the value of slip at full load is about 2% - 6%. The small % slip present manifests itself as sidebands around the 1 times and 2 times RPM components.

6.7.2.3 Speed (Hargis (34))

The torque speed relationship for a motor with a broken bar oscillates at twice slip frequency between the two limits

shown in Figure 6.9. This is because the torque - speed characteristic is normal when the broken bar would not be carrying current if it were intact, but a moment later the bar should be contributing its maximum torque and the characteristic shows that the overall torque is reduced. When quantifying the resulting change in speed it is convenient to assume that the torque contribution from the broken bar completely disappears and that the inertia of the motor and its load is small. Instead of considering changes in speed it is better to use the normalised quantity slip. For a motor with N rotor bars, one of which is broken, the fractional change in slip can be shown to be:

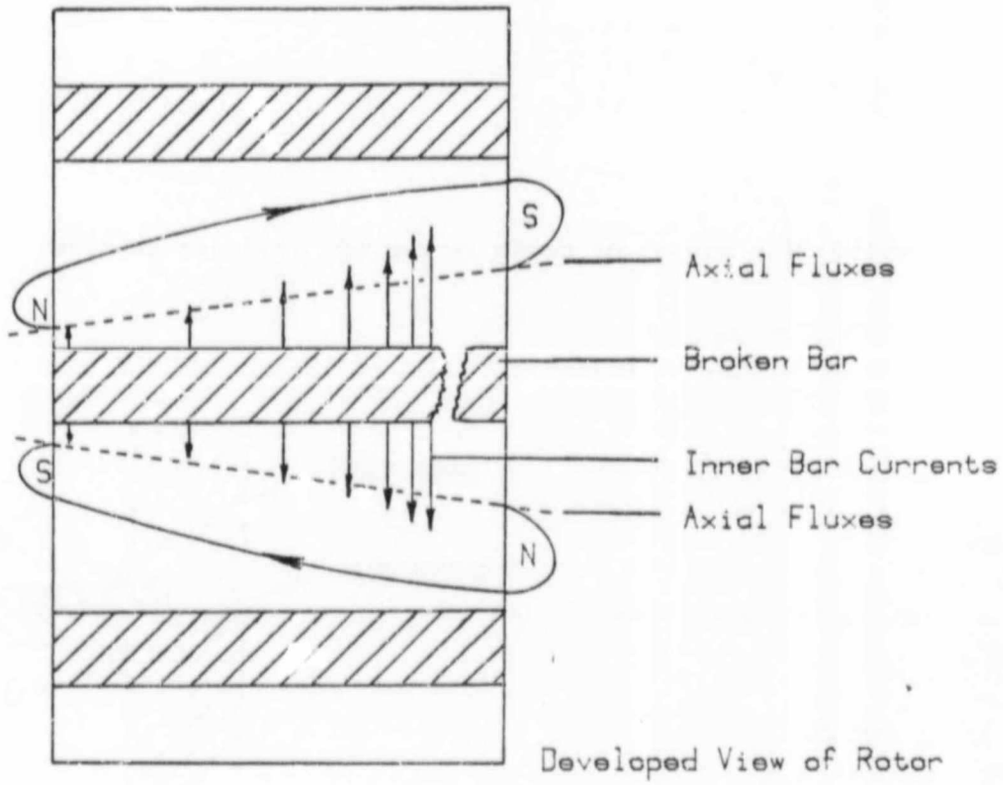
$$\Delta \text{slip}/\text{slip} = 2/N$$

6.7.3 Reasons for Rotor Bar Breakage

The reasons for rotor bar breakage that are discussed here arise from the author's discussion with:

a) Siemens and GEC
b) Power station maintenance personnel
c) Professor C. F. Landy at the University of the Witwatersrand.

1) During the manufacturing process it is normal to weld the rotor bars to the two end rings. The end rings and the bars are heated prior to being welded so that the



AXIAL FLUXES PRODUCED BY INNER-BAR CURRENTS

FIGURE 6.8

TORQUE SPEED CHARACTERISTICS OF SQUIRREL CAGE INDUCTION MOTORS

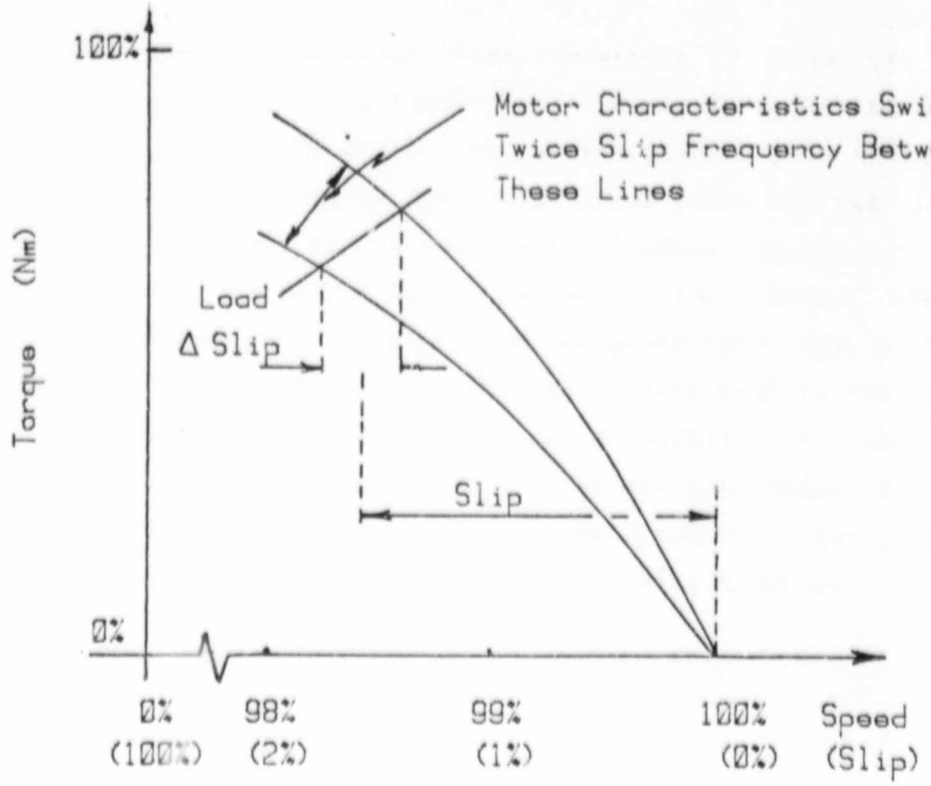
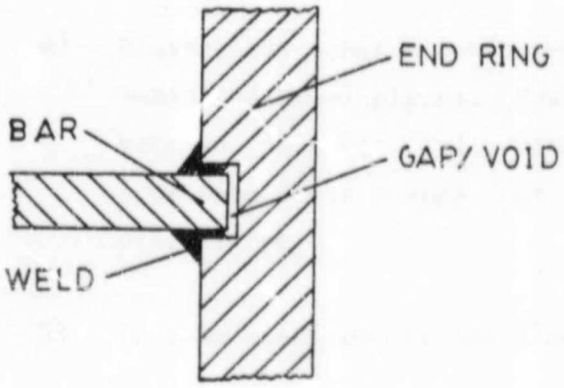


FIGURE 6.9

welding can fill the gap as shown in Figure 6.10 below.



BAR AND END RING WELD FIGURE 6.10

Sometimes the welding does not fill the gap, leaving a void which results in large currents flowing in the reduced welded joint. This in turn leads to overheating.

c) When transmission lines are struck by lighting, it is possible for a flash-over to occur from the transmission line to the earth. In power stations and industry in general this is manifested as an earth leakage problem. When this occurs the earth leakage protection system terminates the supply current to the motor. When the flash-over is terminated the protection system can no longer detect a problem and reverts back to the original status, i.e. current is again supplied to the motor. This all takes place in a few milli-seconds. The motor therefore experiences a large negative torque which can give rise to rotor bar and coupling breakage.

3) Switching the motor on and off repeatedly, results in large induced currents in the rotor bars which are dissipated as heat. This heat induces large stresses in the rotor between the end rings and the cooling rings.

4) Flashes can occur between rotor copper bars and the laminated steel plates. Weak spots are then created between the bar end plate which decreases the cross-sectional area of the bar resulting in overheating.

5) In some cases rotors are simply badly designed.

6.8 VIBRATION MONITORING CRITERIA FOR EARLY DETECTION OF TURBINE ROTOR CRACKS

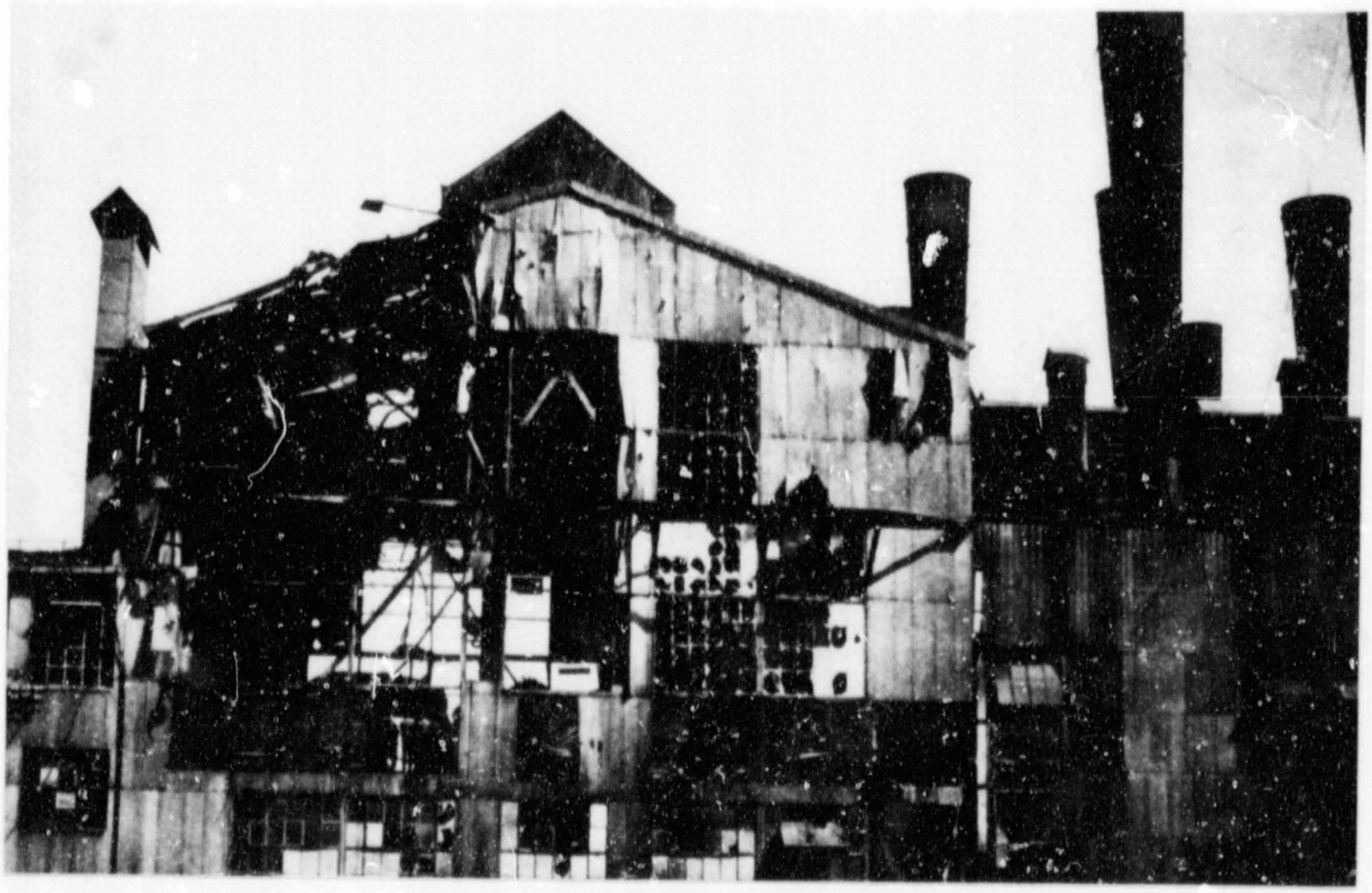
6.8.1 Introduction

Turbo-generator shaft cracking is a serious problem of concern to turbo-generator manufacturers and power supply utilities. In spite of steadily improved materials and methods of stress analysis, new incidents of cracked rotors still occur throughout the world. Several examples include I.P. rotor shafts in the 500 MW turbines at Ferrybridge "C" Power Station during the period May 1972 to March 1974, the I.P. rotor coupling in the 650 MW turbine at Cumberland Steam Plant in September 1976 and the Tennessee Valley Authority Gallatin Unit 2 turbine burst. ESCOM is no exception - examples are, cracked generator rotor at Camden, cracked turbine rotor at Kriel and a cracked turbine rotor at Vaal Power Station. Figure 6.11 illustrates the destructive power of a cracked rotor. These photographs, taken in 1939 at the old Vaal Power Station show the buildings after the turbine disintegrated as a result of a cracked rotor.

Since the consequences of catastrophic failure are very serious, every precaution must be taken to ensure such failures are avoided. Since the vibration pattern of the rotor reflects most mechanical changes in the rotor system it also offers the best means of monitoring a propagating crack.

6.8.2 Vibration Monitoring Criteria

Most critical machines within ESCOM are equipped with a standard safety-related vibration measurement system.



CRACKED ROTOR - OLD VAAL POWER STATION.



FIGURE 6.11

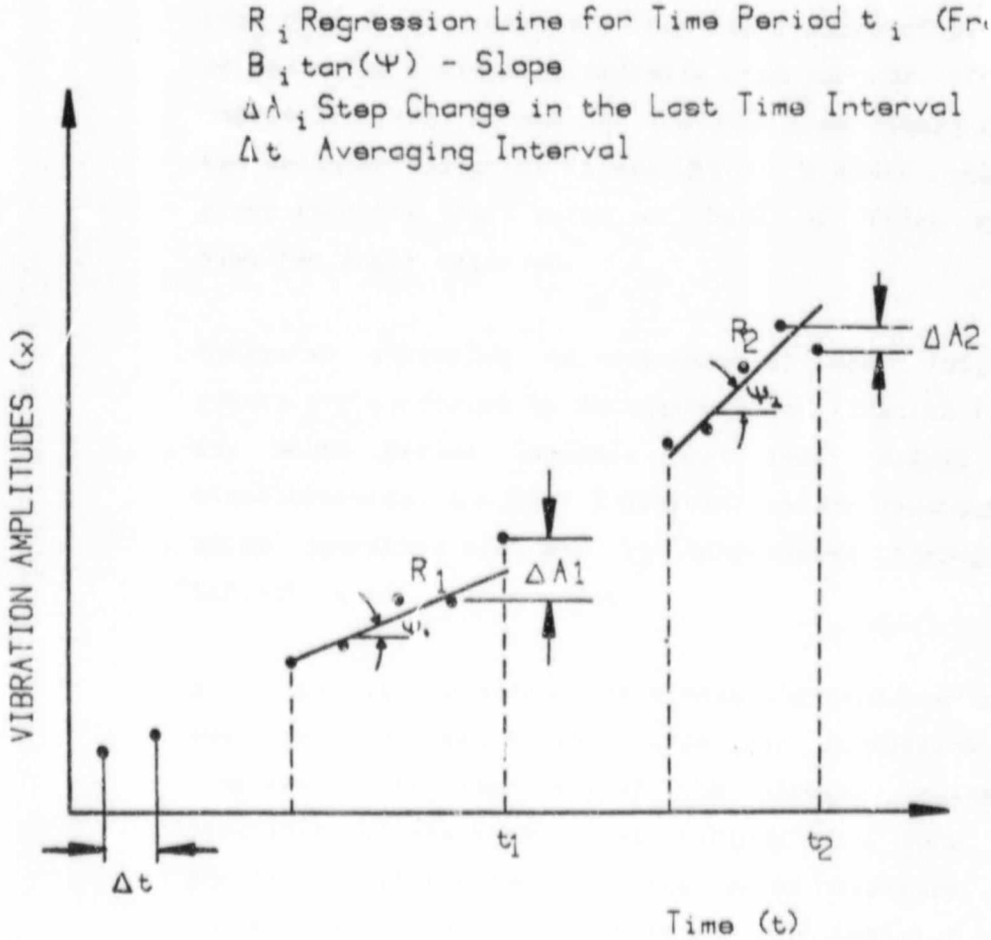
Turbo-generator sets have one vertical seismic probe on each bearing pedestal. The main feedwater pump has two proximity probes located $\pm$ 45° from the vertical at each bearing. The draught group fans have one horizontal velocity transducer on the ND and NDE bearing pedestal. These systems have alarm and trip functions for specified levels of vibration.

The smooth operation of these machines, is altered through many influences which originate from operating procedures and operational disturbances as well as from the appearance of rotor cracks. Since the vibration monitoring equipment has proven satisfactory over many years of safe machine operation, it is the author's view that it would be advantageous to utilise this same equipment to detect cross-sectional cracks.

Accurate knowledge of the natural vibration amplitude changes caused by external influences such as back pressure and various operating conditions, is undoubtedly an important pre-requisite for the formulation of the transverse crack detection criteria. A specific "dead band" of vibration amplitude changes must be interpreted as normal and thus allowed.

To eliminate spurious fluctuations, it is necessary to formulate mean values from measured vibration values, perhaps on a daily basis. This procedure of averaging the values does not overshadow the expected amplitude change following the formation of a transverse crack, since the laws of crack propagation can be applied over longer periods of time, for instance over several days or weeks. The amplitude changes are progressive as the relative crack depth grows.

This behaviour has to be incorporated into the crack indicating criteria in which a regression curve is determined as shown in Figure 6.12, from the averaged measured values over a given time interval.



SCHEMATIC REPRESENTATION OF THE CRACK-INDICATING CRITERIA FOR A TURBINE-GENERATOR

FIGURE 6.12

The progressive change is obtained from the difference in the last two amplitudes, which likewise must exceed a given value. Mean derivation final step change in amplitude and

time interval for the regression calculations must be so adapted as to not only eliminate false indications caused by the aforementioned operating influences, but also to incorporate the required sensitivity to ensure timely detection of transverse cracks before the occurrence of serious damage.

As depicted in Figure 6.12, the regression curves for a given time period are determined from the average of five measured values. The monitoring criteria used are the slope of the regression line, B_i and the absolute step change in the last two measured vibration values (ΔA_i). A crack indication is given when the limit value for both of these criteria is simultaneously exceeded.

Extensive vibration measurements of many large turbine generators performed by Baumgartner and Ziebarth (35) over a two month period indicate that limit values $B_2 = 5$ micrometers/day and $\Delta A = 5$ micrometers are reasonable so that normal operation will not be interrupted through a false indication of a rotor crack.

A propagating transverse crack normally causes changes in the once per revolution and twice per revolution vibration components. The magnitude of the changes depends on the senstivity of the rotor to excitations with once and twice per rotational frequency in the axial position where the crack is situated and of course on the position where the vibration components are measured. There can also be changes in the three times rotational frequency and higher order vibrations, but in normal turbo-generators these vibrations are more heavily damped and therefore of less interest.

It is very important to consider vector changes of vibration and not only changes in vibration amplitude which could be considerably smaller due to phase shift.

The existence or growth of a crack can be detected from the vibration of the shaft when running below the main critical speed provided that the mode shape corresponding to the critical speed is such as to cause a bending moment at the section containing the crack.

During coastdown, advantage can be taken of the dynamic magnification of vibration components at the shaft critical frequency. In the case of horizontal shafts balanced to ISO 1940 (36) the combination of gravity and a crack will result in a resonance at the main critical speed which will dominate the resonance due to out-of-balance. Henry (37) suggests this will occur when the crack factor has reached about 2%.

$$\text{crack factor} = (w_1 - w_2)/w_2$$

where w_1 and w_2 represent the natural angular frequencies of the shaft in the x and y directions respectively.

6.9 SHAFT ORBITAL ANALYSIS

6.9.1 Introduction

The use of proximity probes for measuring the dynamic motion of rotating machinery has gained universal acceptance. An important aspect in determining the mechanical integrity of a rotating system involves the measurement of shaft relative motion. Since the proximity probe is essentially a DC

voltage versus gap transducer, the shaft position measurement is provided using the DC voltage while the dynamic motion measurement is provided using the AC voltage.

Shaft orbital analysis employs two proximity probes, at each bearing, located $\pm$ 45° from the vertical.

A pair of probes can determine the shaft position at any instant. Signals from these probes are coupled to an oscilloscope which displays this position visually. A third proximity probe can read out the angular position of the shaft at its maximum deflection. This probe is mounted in some convenient plane and signals the passage of a timing mark on the shaft. A keyway or key on the shaft makes a good timing mark. The output from the keyphasor probe is coupled to the oscilloscope's beam intensity input. As the mark passes the probe a bright spot appears on the orbit display to indicate vectorially which way the shaft deflects at that instant.

The most common machinery vibration problems are shaft related e.g. imbalance rubs, misalignment and oil instability. Shaft measurements are generally more reliable than shaft absolute motion measured on the bearing pedestal, for overall machine protection monitoring systems or periodic machine measurements. They provide more meaningful information than shaft absolute motion for malfunction diagnosis. Many rotating machines, particularly those with fluid film bearings and large casing to rotor mass ratios, generate much more shaft motion relative to the bearing or bearing housing than absolute bearing casing motion.

The only major limitation when using proximity probes concerns the quality and nature of the shaft surface to be observed. Ideally, the probe should observe a surface equal in finish to the shaft bearing journal. Surface imperfections such as scratches, dents, rust and out-of-roundness produce mechanical runout, which appears as a noise component on the output signal of the probe. In addition, the proximity transducer system is affected by changes in magnetic and conductive properties of the shaft surface material. If surface conductive (resistivity) properties change significantly from one point on the shaft circumference to another, this may also cause electrical runout. Such changes in surface resistivity may originate from metallurgical changes, surface hardness variations, heat treatments, certain grinding finishing techniques and plating or spray metalising processes. Slow roll vector subtraction and surface treatment can be used to solve mechanical and electrical runout problems respectively. Slow roll vector subtraction stores the profile of the shaft with its dents, scratches and out of roundness at a "slow-roll" speed of approximately 100 RPM. Since out of roundness, scratches and dents will manifest themselves as a vibration problem, it is necessary to eliminate this false vibration. This is exactly what slow roll vector subtraction achieves. Slow roll vector subtraction subtracts the profile of the shaft at the "slow-roll" speed from the absolute shaft vibration at the operational rotational speed of the machine.

Data obtained from proximity probes can be in the form of transient and steady state data. Typically, transient data is acquired during machine start-up or coastdown when rotor speed is changing as a function of time. Steady state data is acquired when the machine is at a constant operating condition, such as constant rotor speed, flow and load.

The Tutuka, Lethabo and Matimba feed pumps, at ESCOM's new power stations, will have two permanently installed proximity probes mounted at each bearing. They will also have a fifth permanently installed proximity probe which will be used a a keyphasor reference. Since the pumps have the five permanently installed proximity probes each, for periodic monitoring, shaft orbital and phase analysis can be performed by the maintenance personnel.

6.9.2 Shaft Orbital Analysis Using Steady State Data

Since an orbit is an exact representation of dynamic shaft motion, this display can be very informative of mechanical condition and the presence of specific malfunctions. Additional information can be obtained by introducing a phase-indicating mark on the wave form of the orbit.

Orbits and the corresponding time base plots for various malfunctions are illustrated in Figure 6.13.

To make the interpretation of transient shaft orbits less confusing it was decided by the author to simulate shaft orbits using a computer. A computer programme was generated to simulate shaft orbits for varying phase angles and, vertical and horizontal magnitudes. Figure 6.14 shows shaft orbits with varying magnitudes and phase angles. These orbits can be very useful in determining the magnitudes of the vertical or horizontal vibration components as well as the phase angle between these two components. Figure 6.15 shows typical orbits with equal vertical and horizontal components but varying phase angles. The phase angles vary from 0^{o} to 180^{o}.

ORBITS & TIME BASE PLOTS FOR VARIOUS MALFUNCTIONS

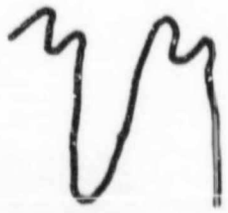
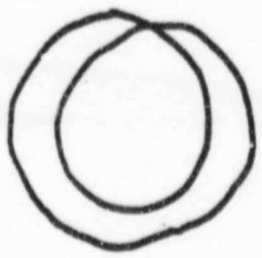
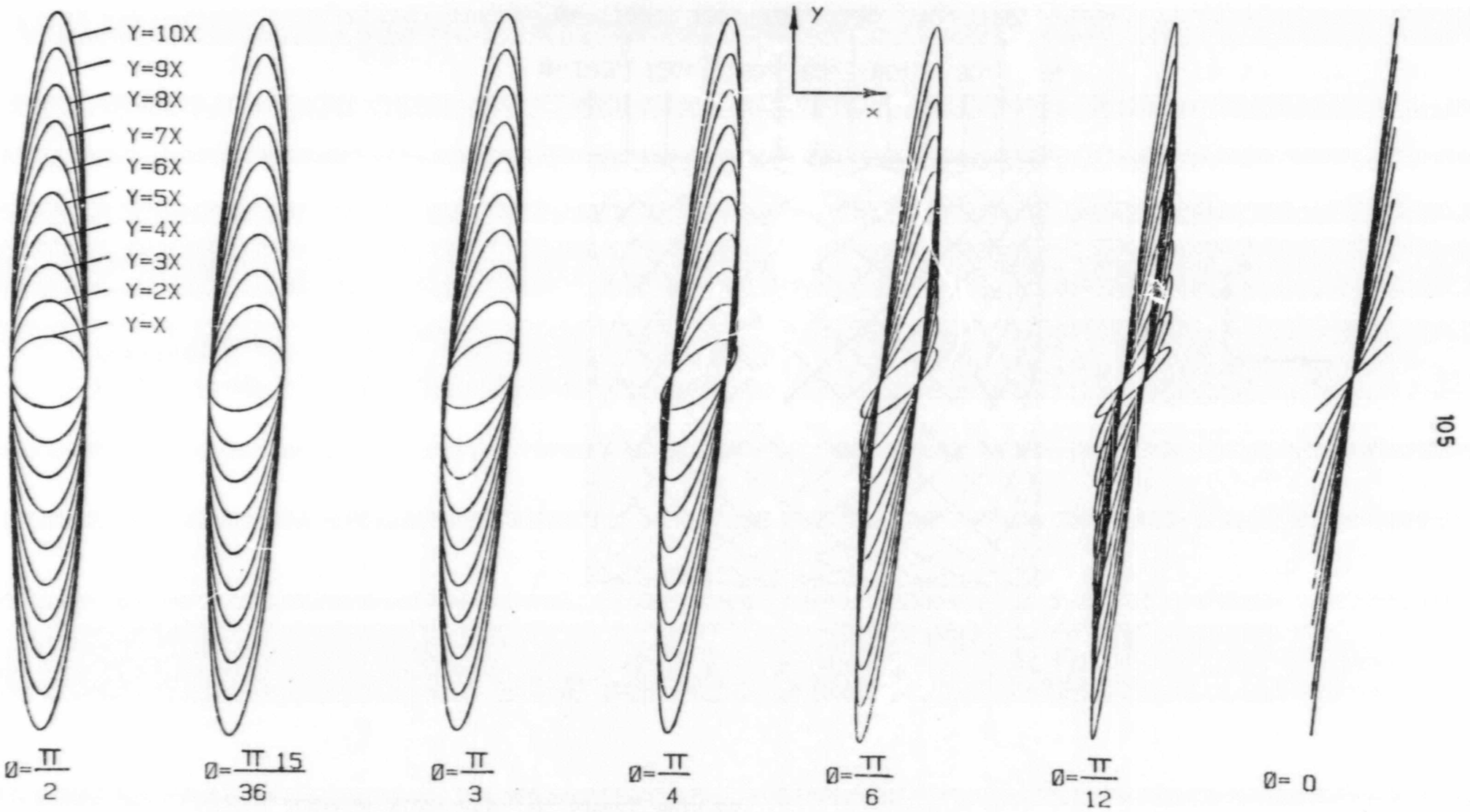
MALFUNCTION	TIME BASE	X-Y PLOT	DIAGNOSIS
MISALIGNMENT			TYPICAL OF SEVERE MISALIGNMENT
OIL WHIRL			WHIRL FREQUENCY < 0,5 SHAFT SPEED
RUB			CONTACT PRODUCES SPIKE SUPERIMPOSED ON NORMAL ORBIT
UNBALANCE OR BENT SHAFT			OVAL X-Y PLOT

FIGURE 6.13

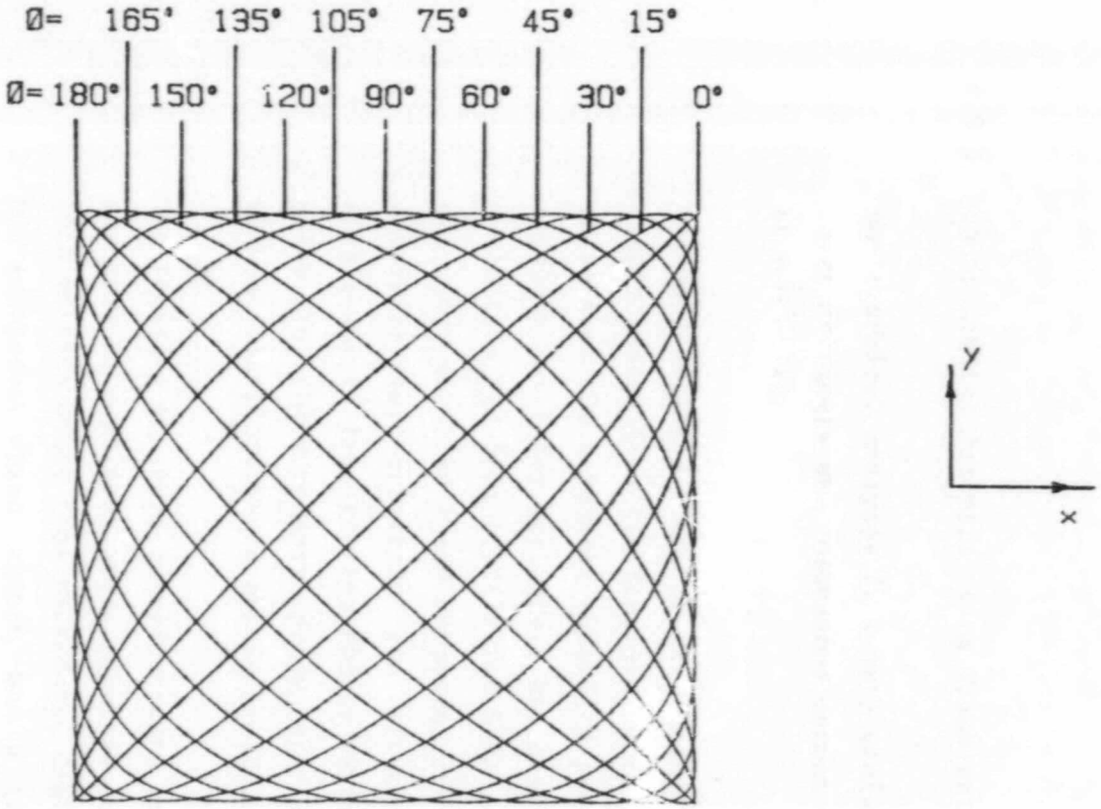
SHAFT ORBITS WITH VARYING MAGNITUDES AND PHASE ANGLES.



$x = X\sin(wt)$

$y = Y\sin(wt+\emptyset)$

FIGURE 6.14



$x = X\sin(wt)$

$y = Y\sin(wt+\emptyset)$

$X = Y$

SHAFT ORBITS WITH VARYING PHASE ANGLES.

FIGURE 6.15

6.9.3 Shaft Orbital Analysis Using Transient Data

Shaft orbital analysis is a very useful tool for determining shaft criticals and resonances during a start-up or coastdown of a machine.

Normally during a start-up or coastdown of a machine the displacements from the four proximity probes as well as the pulse from the keyphasor proximity probe are stored on a tape recorder for later analysis. The analysis of the above data would take the form of filtered Bode and Nyquist plots of the one times rotative speed component and harmonics thereof, to determine shaft criticals and structural resonances. The displacements from the two NDE or DE proximity probes and the pulse from the keyphasor probe can be viewed on a dual channel oscilloscope to obtain orbits.

The facility to store transient data and to perform detailed analysis as mentioned above requires sophisticated equipment, like multi-channel tape recorders, digital vector filters and FFT analysers, which cannot be duplicated at each power station. Even without sophisticated equipment the maintenance personnel at the power station will still be able to perform limited transient data analysis.

If a speed indicator is available and the orbits are carefully viewed on the oscilloscope shaft criticals and resonances can be approximately determined. Shaft criticals and resonances are characterised by maximum vibration amplitude coupled with a phase change. By noting the speed, on the speed indicator, at which this phenomenon occurs one can obtain the shaft criticals or structural resonances. It was decided by the author to generate transient shaft orbits with varying horizontal and vertical stiffness ratios.

The reasons for generating these orbits were:

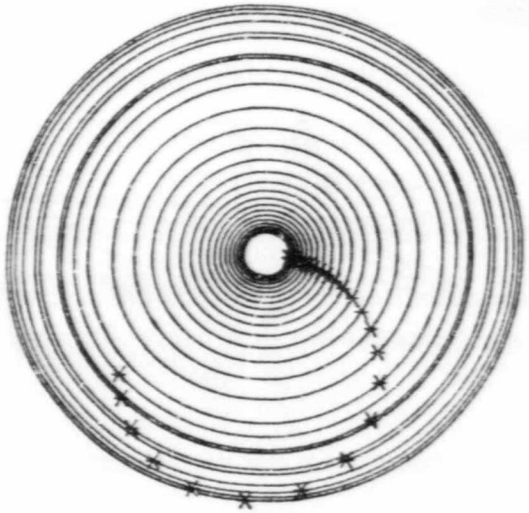
a) It is very difficult to ascertain phase changes and maximum vibration amplitudes, accurately on an oscilloscope during a run-up or coastdown of a machine.

b) Unless a keyphasor is visible on the orbit it is difficult to determine shaft criticals or resonance.

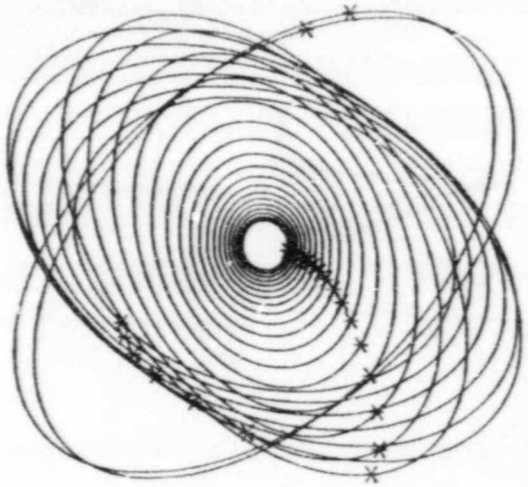
c) It is advantageous to see the variations of the magnitudes of the orbits and the changing of the keyphasor during a run-up or coastdown of a machine, all on one plot.

Typical computer predicted transient shaft orbits from a start-up or coastdown with varying horizon and vertical stiffness ratios can be seen in Figures 6.16 and 6.17.

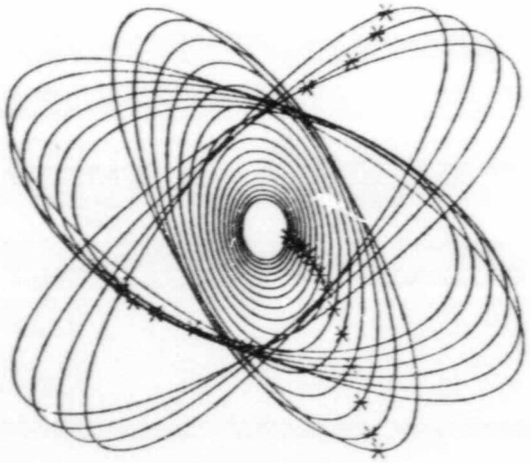
When ky = 0,8 kx the orbits start off in an elliptical fashion, reach a maximum at w_n^2 = ky/m and change phase. The same procedure is repeated at w_n^2 = kx/m. (See Appendix 2 for the derivation of these shaft orbits). These are typical orbits that one could expect when passing through a critical or resonance. Notice that when the horizontal and vertical stiffnesses are the same there is only one resonance, but when the stiffnesses are unequal then two resonances exists.



$k_y = k_x$



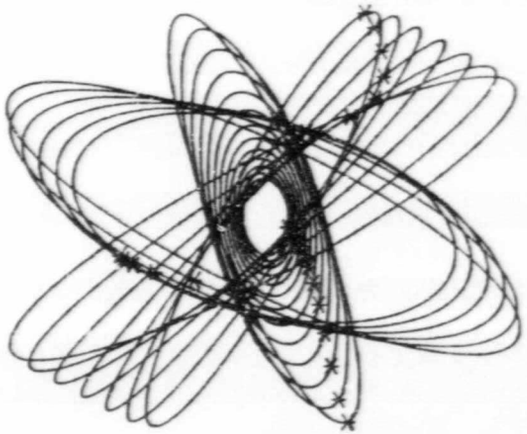
$k_y = 0.9k_x$



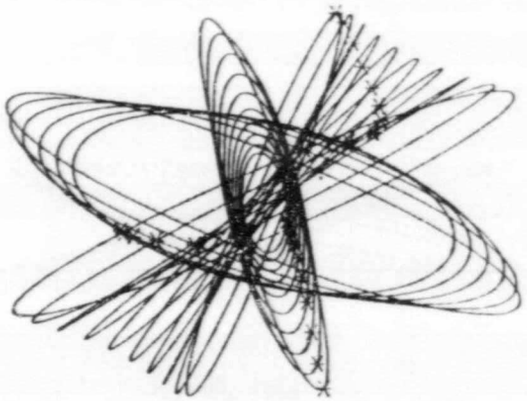
$k_y = 0.8k_x$

SIMULATED SHAFT ORBITS FOR DIFFERENT HORIZONTAL AND VERTICAL STIFFNESS RATIOS.

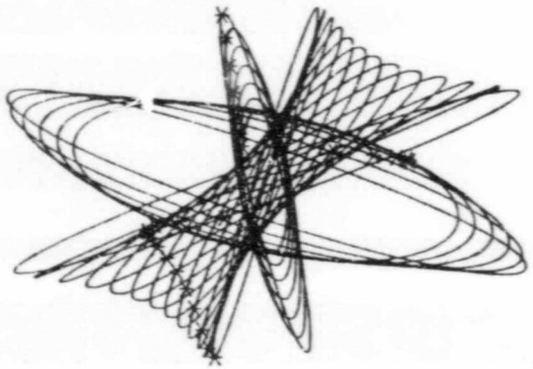
* KEYPHASOR REFERENCE



$k_y = 0.7k_x$

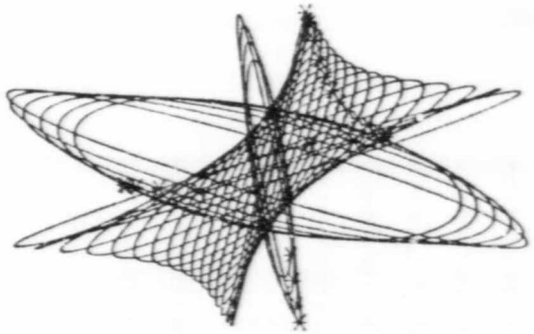


$k_y = 0.6k_x$

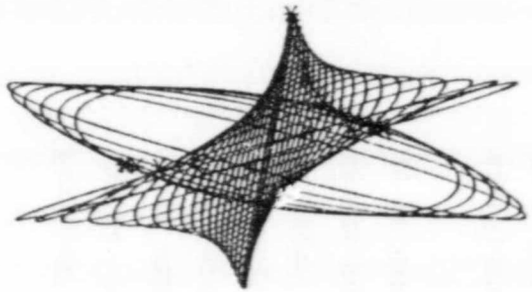


$k_y = 0.5k_x$

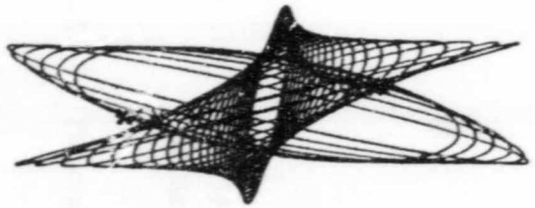
FIGURE **6.16**



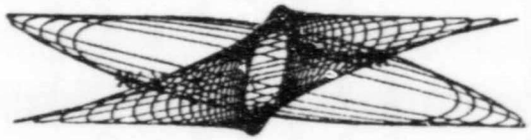
ky=Ø, 4kx



ky=Ø, 3kx



ky=Ø, 2kx



ky=Ø, 1kx

FIGURE 6.17

6.10 DIAGNOSIS OF SUB-SYNCHRONOUS ROTOR DYNAMIC INSTABILITIES USING SHAFT ORBITAL ANALYSIS

6.10.1 Introduction

Two of the most important energy transformers on rotating machinery are the oil whirl and oil whip phenomena. The oil whirl energy transformer mechanism may express itself in any non-compressible fluid bearing or quasi-bearing wherein the shaft surface drags the lubricating fluid around in the direction of rotation.

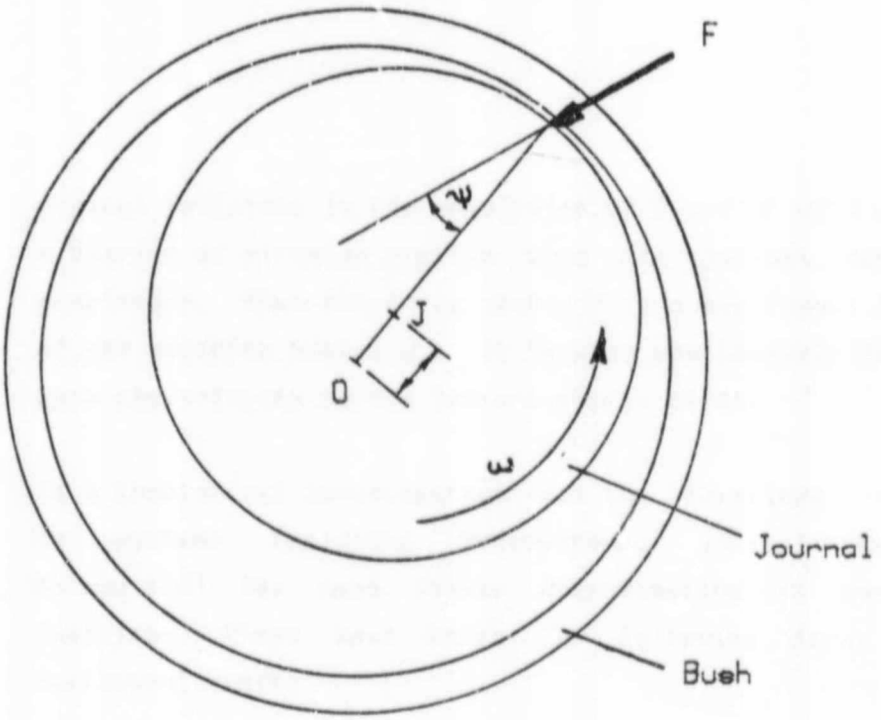
It is necessary to maintain an oil film for prevention of direct contact between the rotating surface and non-rotating surface. The oil film also assists in removing dissipated energy from the bearing area. However, it is exactly this fluid drag mechanism which can act as the energy transformer which may under certain conditions, convert useful torque energy into energy devoted to creating radial dynamic orbiting, forward whirl or whip of the rotor system.

6.10.2 Theory Holmes (38)

Often shafts are supported by oil-lubricated journal bearings, the load carried by hydrodynamically-generated pressures in the oil film. With reference to Figure 6.18 if a journal of this type of bearing is rotated at a constant angular velocity , about its own centre, the centre being fixed at a distance ϵ from the bush centre, it will experience a constant force F at angle ψ to the displacement ϵ.

The magnitudes of the force F and the angle ψ depend upon the eccentricity ratio $\eta = \epsilon/c$. Figure 6.19 illustrates a

SCHEMATIC REPRESENTATION OF JOURNAL AND BUSH



c= Mean Clearance

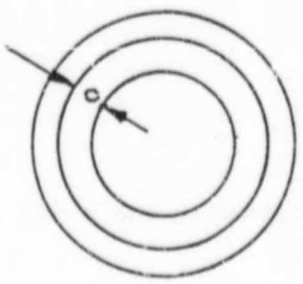


FIGURE 6.18

TYPICAL VARIATION IN MAGNITUDES OF F AND ψ WITH ε.

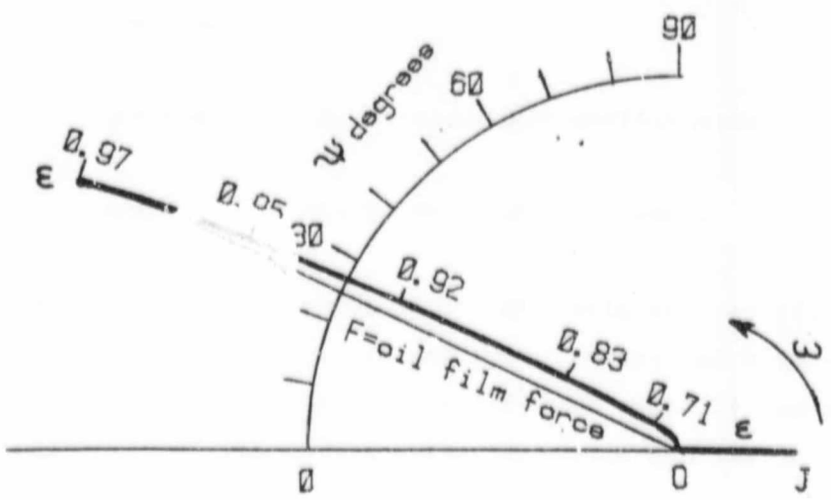


FIGURE 6.19

typical variation in the magnitudes of F and ψ with η, for a bearing of circular profile when the journal centre is stationary. Thus the force vector F is a non-linear function of the position vector $\bar{\varepsilon}$. It is also non-linearly dependent upon the velocity of the journal centre $d\bar{\varepsilon}/dt$.

In a theoretical investigation into the vibrations occurring in systems employing hydrodynamic journal bearings, Holmes (38) has used linear approximation to non-linear functions. These have taken the following form, for a horizontal shaft:

$$\begin{bmatrix} Fx \\ Fy \end{bmatrix} = \begin{bmatrix} Fox \\ Fay \end{bmatrix} + \begin{bmatrix} axx & axy \\ ayx & ayy \end{bmatrix} \begin{bmatrix} x \\ y \end{bmatrix} + \begin{bmatrix} bxx & bxy \\ bxy & byy \end{bmatrix} \begin{bmatrix} \dot{x} \\ \dot{y} \end{bmatrix} \qquad (6.1)$$

where:

Fx,Fy are the x and y components respectively of force F.

Fox,Foy are the values of Fx and Fy when the journal centre is stationary at its steady running position.

x;y are small displacements from the steady running position.

aij are known as the displacement coefficients.

bij are known as the velocity coefficients.

The values of the displacement and velocity coefficients depend upon many factors, including the shape and size of the bush and journal surfaces, the rotational speed of the shaft, the viscosity of the oil, and the magnitude and direction of the steady load.

The small amplitude motion, about its steady running position, of a symmetrical shaft of bending stiffness k, when supported in two hydrodynamic journal bearings and carrying a mass M at its mid-span, is governed by the following equations of motion:

$$M\ddot{x} + k(x - x_1) = Mw^2 h\,Cos\,(wt) \qquad (6.2)$$

$$M\ddot{y} + k(y - y_1) = Mw^2 h\,Sin\,(wt) \qquad (6.3)$$

where:

x,y — are the co-ordinates of the shaft axis at mid-span relative to its steady running position.

$x_1; y_1$ — are the co-ordinates of the shaft axis at the journal, relative to its steady running position.

h — is the radius of the mass centre from the shaft axis at mid-span.

A force balance on the journals gives

$$k(x - x_1) = a_{xx}x + a_{xy}y + b_{xx}\dot{x} + b_{xy}\dot{y} \qquad (6.4)$$

$$k(y - y_1) = a_{yx}x + a_{yy}y + b_{yx}\dot{x} + b_{yy}\dot{y} \qquad (6.5)$$

In general, even for a perfectly circular bearing the oil film characteristics are unsymmetrical, so we should expect two natural frequencies for each shaft speed and for each the whirl frequency which coincides with the natural frequency. Consequently, we should expect two resonance type critical speeds in which the whirl velocity coincides with the shaft velocity. This condition is referred to as synchronous

whirl. However, there are two complicating factors which prevent the system behaving completely in this manner:

a) for a particular system, under a particular steady load there is a rotation speed above which the free motion is unstable, because the system damping becomes negative.

b) when the amplitude becomes large, as at resonance, the linearised equations (6.1) do not hold.

The unstable motion arising from the oil film forces was first reported by Newkirk and Taylor (39). They referred to the phenomenon as "oil whip", and reported that the vibration or whirling frequency bore little, if any, relation to the shaft speed and that the phenomenon was practically independent of balance. More recent investigations by Pinkus and Tondl (40) and (41) respectively indicate that the ratio of free whirl velocity to shaft velocity takes values which decrease from about 0,5 when the shaft velocity is much less than twice the lowest natural angular frequency. The whirl velocity takes the value of the lowest natural angular frequency of the rotor when the shaft velocity is greater than twice that value. That is, for a rigid rotor the free whirl velocity is about half the shaft velocity. This condition has been called "half-speed whirl" or "sub-synchronous whirl".

The speed at which this action takes place is defined in the following manner. The velocity of the rotor film at the non-rotating surface of the bearing is zero. The velocity of the oil film at the rotating surface of the shaft in the bearing is the velocity of the surface. Assuming laminar

flow, the oil between must be travelling with the velocity distribution as shown below in Figure 6.20.

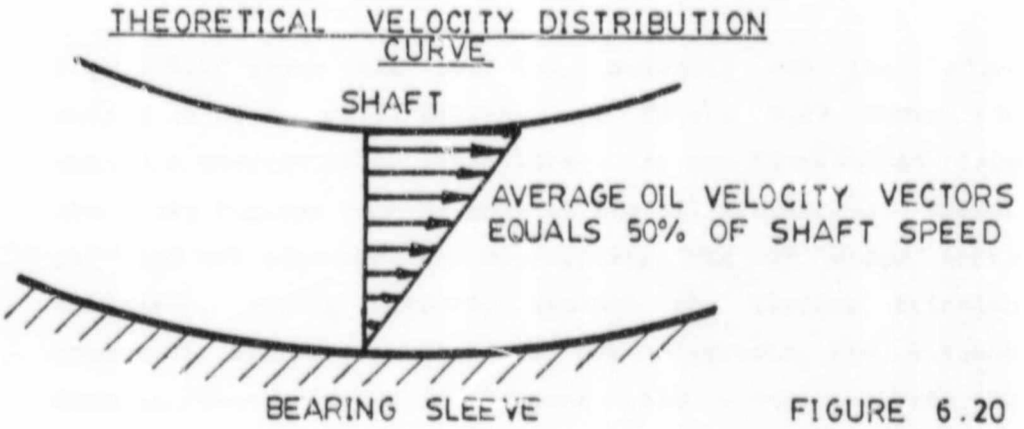


FIGURE 6.20

On the assumption of triangular velocity distribution, the forcing function travels at 50% of rotative speed, in the forward direction of rotation.

Experimental evidence, however, overwhelmingly demonstrates that the pure oil whirl mechanism is strongly preferential at between 42% and 48% of rotative speed. The main reason for the speed rate being lower than the theoretical 50% is obvious when it is recognised that the rotating surface is usually the shaft and the shaft surface is usually smooth. The usual bearing non-rotating surface is relatively rough. This leads to the oil velocity distribution across the clearance area, as shown in Figure 6.21.

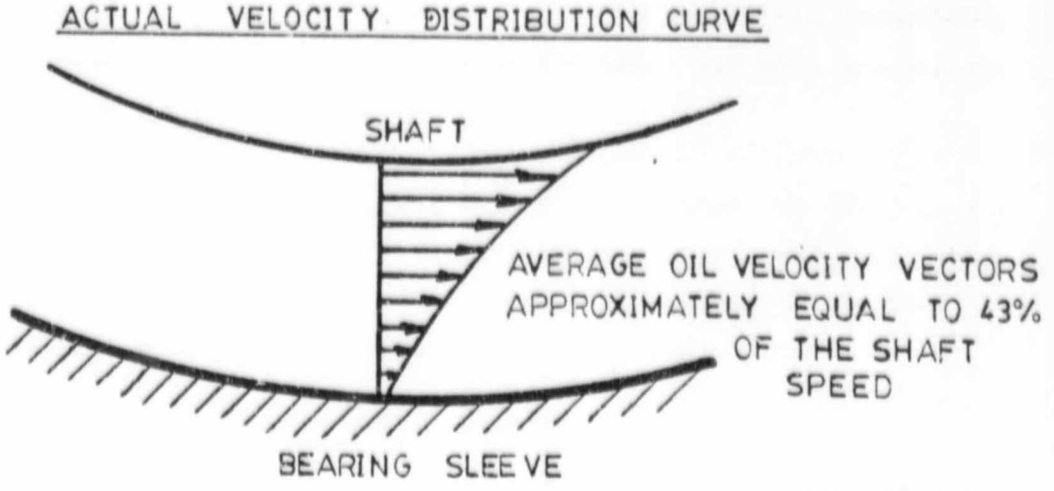


FIGURE 6.21

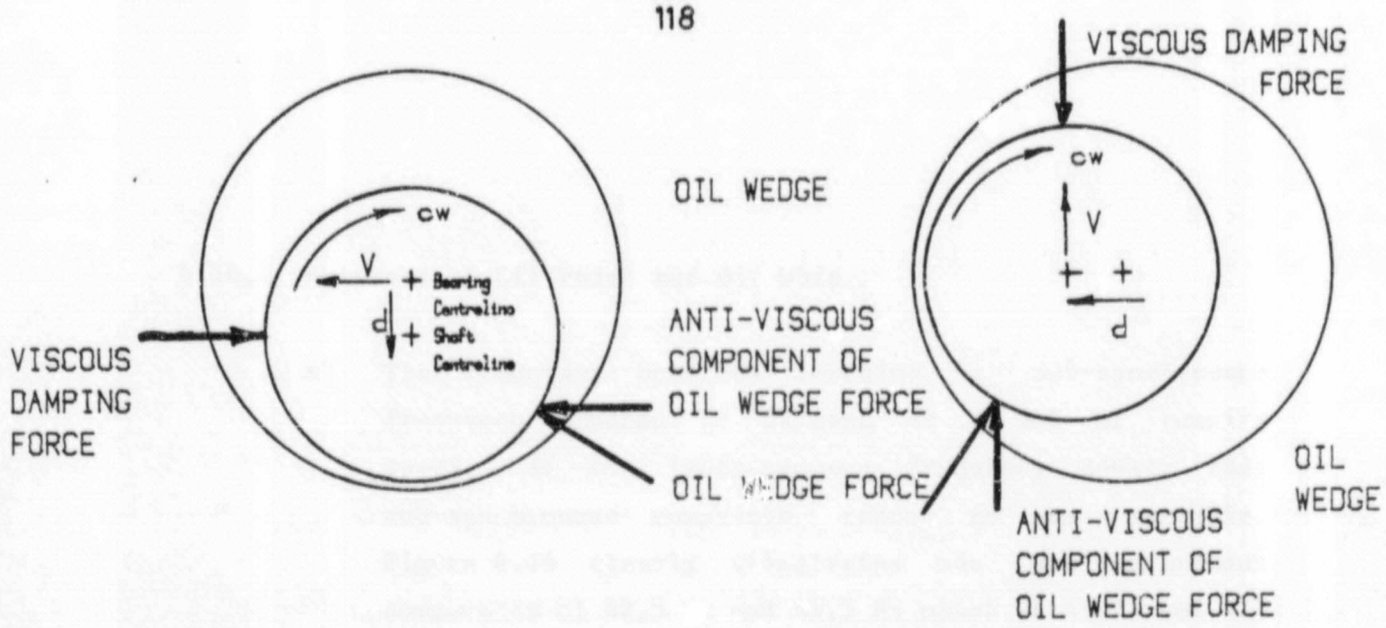
The average oil velocity with this concave distribution is less than 50%.

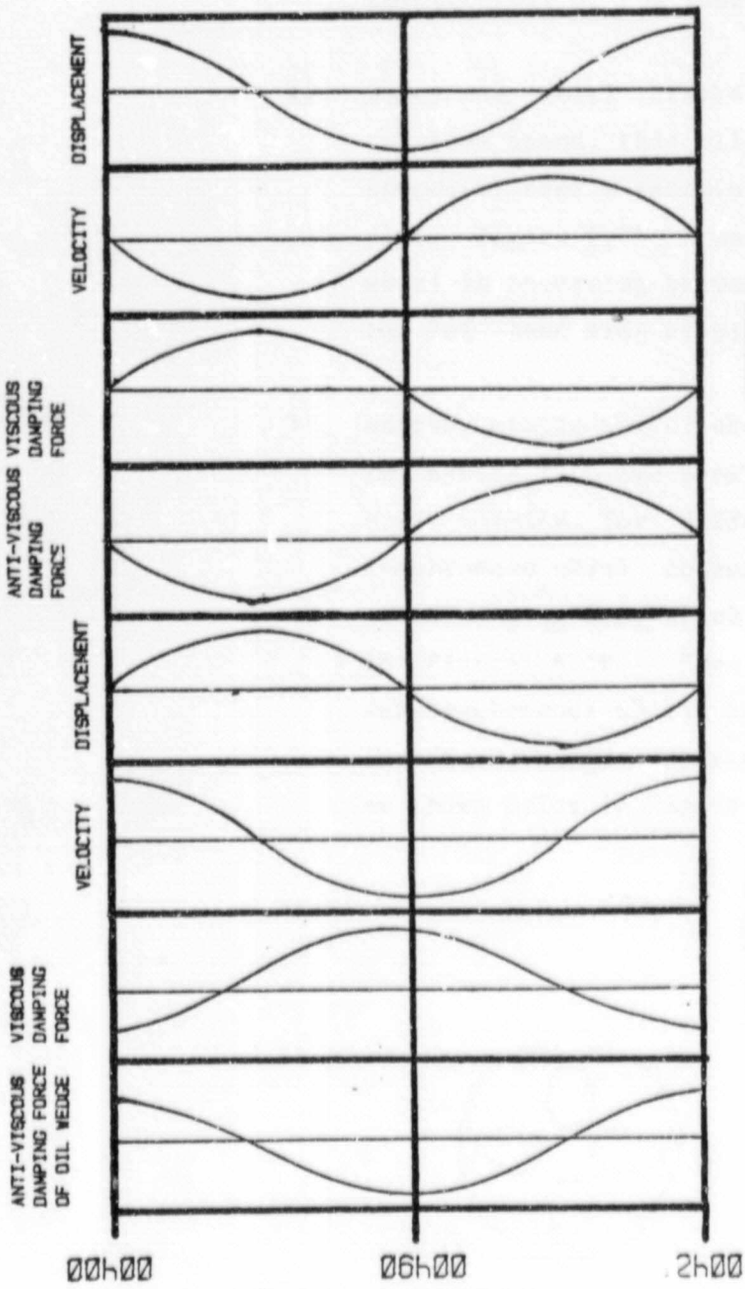
Figure 6.22 shows the position, velocity and the forces acting in an oil whirl action, and Figure 6.23 shows the action a quarter of an orbit later. It may be observed from the above Figures that as soon as the oil properties, speed, pre-load and clearance are appropriate, the oil wedge force component, acting directly against the viscous friction component, overcomes but does not eliminate the viscous damping force. Once this happens, the rotor proceeds to vibrate at whatever average speed the oil film circulates, usually near 43% of the shaft rotative speed, and in a forward circular orbit. This mechanism is presented in theoretical form by Kirk et al (42).

Lacking any influence other than average oil velocity, the oil whirl tracks a fairly constant ratio of rotative speed. If the rotor system has a resonance below rotative speed such as a balance resonance, oil whirl and resonance inter-act with each other. When this occurs it is called oil whip.

Most of the critical machines in a power station have sleeve bearings, e.g. the main turbo generator set, the steam and electric feedwater units and the draught group fans. Oil whirl and whip could become a problem in these machines, and hence it is vitally important that a condition monitoring team knew what the symptoms of oil whirl and whip are and how to diagnosis the problem.

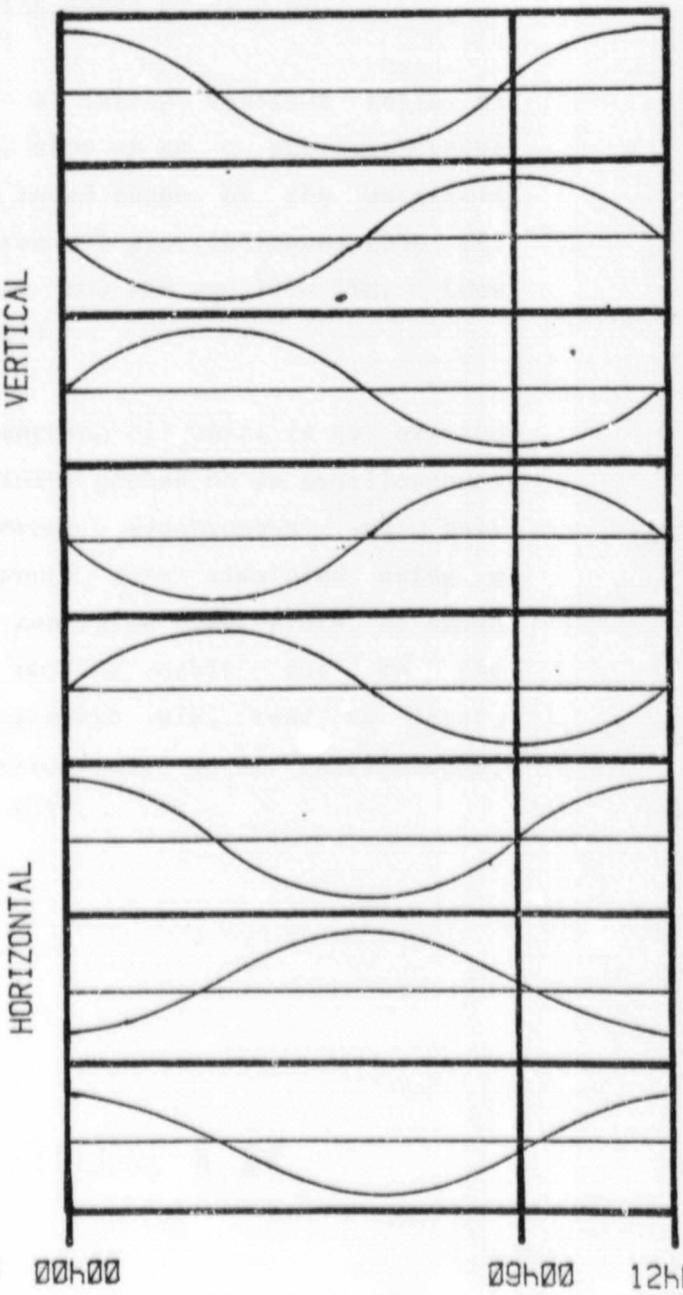
Detailed tests were performed by the author on the Bently Nevada rotor kit to simulate oil whirl and oil whip. Spectrums, orbits and waterfall plots were obtained to demonstrate the symptoms of oil whirl and whip.





OIL WHIRL : SHAFT AT 06H00

FIGURE 6.22



OIL WHIRL : SHAFT AT 09H00

FIGURE 6.23

Author Ducci PP
Name of thesis Vibration Analysis And Diagnostic Techniques, With Reference To The Implementation Of A Vibration Condition Monitoring Programme. 1987

PUBLISHER:
University of the Witwatersrand, Johannesburg
©2013

LEGAL NOTICES:

Copyright Notice: All materials on the University of the Witwatersrand, Johannesburg Library website are protected by South African copyright law and may not be distributed, transmitted, displayed, or otherwise published in any format, without the prior written permission of the copyright owner.

Disclaimer and Terms of Use: Provided that you maintain all copyright and other notices contained therein, you may download material (one machine readable copy and one print copy per page) for your personal and/or educational non-commercial use only.

The University of the Witwatersrand, Johannesburg, is not responsible for any errors or omissions and excludes any and all liability for any errors in or omissions from the information on the Library website.